Influence of H^+ and Calcium Ions on Surface Functional Groups of *Synechococcus* PCC 7942 Cells

Maria Dittrich* and Sabine Sibler

Swiss Federal Institute of Aquatic Science and Technology, Eawag and Swiss Federal Institute of Technology, ETH, CH- 6047 Kastanienbaum, Switzerland

Received November 17, 2005. In Final Form: March 13, 2006

The chemistry of the surface functional groups of picocyanobacteria *Synechococcus* PCC 7942 cells was examined as a function of H^+ and calcium concentrations. Titration experiments, infrared spectroscopy, biosorption experiments, and chemical modeling were used to gain insight into the mechanisms of biosorption. The pK_a and concentration of active sites on the cell wall were clarified with the aid of potentiometric titration. Modeling calculations and infrared spectra are consistent with pK_a's values of 4.3, 5.2, 6.9, 9.1, and 10.0 and a total concentration of 7.8×10^{-4} mol g^{-1}. Spectral analysis of an aqueous cellular suspension revealed a presence of carboxyl, amide, phosphate, hydroxyl, and carbohydrate moieties. Correspondence between spectral data and potentiometric titration curves supported the hypothesis that carboxylate groups and phosphodiester groups mediate calcium adsorption to bacterial cells. This process is strongly pH dependent. In the second part of the experimental work, *Synechococcus* cells were suspended in the presence of different calcium concentrations. Mechanistic modeling demonstrated that the calcium adsorption phenomenon can be described taking into account only two mechanisms: ion exchange and complexation.

1. Introduction

The composition and structure of bacterial surfaces is responsible for important processes such as biomineralization, bacterial adhesion, and biofilm formation.[1−4] Although the bulk chemical composition of a bacterial cell is often known, the molecular characteristics of their surfaces are not well characterized.[5,6] Phototrophic picocyanobacteria, who's cells sizes are <2 μm, contribute to around half of the carbon fixed in marine systems.[7] Cyanobacteria of the genera *Synechococcus*[8,9] are abundant in the world's oceans from 50° south to 70° north and play a significant role in metal sorption.[10] Although cyanobacterial picoplankton are often the dominant phytoplankton in terms of biomass,[11] a limited number of studies have examined their influence on the biogeochemical cycling in aquatic systems.

Recent studies indicate that Gram-negative picocyanobacteria also play an important role in calcite precipitation in oligotrophic lakes.[12] One proposed mechanism is a two-step process, during which calcium cations first bind to the cell surface, followed by the diffusion of hydroxyl ions through the cell membrane as a result of an uptake of HCO_3^- by photosynthesis.[13] Although the observation of fast and reversible Ca adsorption on picocyanobacterial cells supported this mechanism,[14] the detailed steps of the precipitation on the cell surface remain unclear.

The deprotonation constants of surface groups of picocyanobacteria are similar to those of other bacterial strains, which have been recently examined using both macroscopic (potentiometric titration, ion adsorption) and molecular (microscopy and spectroscopy) tools.[15−18] Research studies led to the identification of major proton-active functional groups on bacterial surfaces and the development of a series of thermodynamic metal binding constants. More recently with the development of electrostatic and atomic force microscopy,[19,20] attempts to directly inspect and quantify the charge development on cell surfaces have been made. Moreover, in situ methods such as infrared spectroscopy and Raman spectroscopy were used to study the behavior of bacteria−water interfaces, their interactions with various chemicals,[21−23] their variations as a function of cell structure (Gram-positive versus Gram-negative),[18] the process of cell adhesion, biofilm growth, and biomineralization.[24] However, molecular information to support the pK_a's of protonation and complexation of cyanobacteria *Synechococcus* genera remains limited. In our previous study, we characterized the surface

* Corresponding author. Tel.: +41 41 349 21 24. Fax: +41 41 349 21 68. E-mail: dittrich@eawag.ch.

(1) Borrok, D.; Fein, J. B. *Geochim. Cosmochim. Acta* **2004**, *68*, 3043−3052.
(2) Lower, S. K.; Hochella, M. F.; Beveridge, T. J. *Science* **2001**, *292*, 1360−1363.
(3) Beveridge, T. J.; Doyle, R. J. *Metal ions and bacteria*; Wiley: New York, 1989.
(4) Jucker, B. A.; Harms, H.; Hug, S. J.; Zehnder, A. J. B. *Colloids Surf.* **1997**, *9*, 331−343.
(5) Marshall, K. C.; Pembrey, R. S.; Schneider, R. P. *Colloids Surf. B, Biolnterfaces* **1994**, *2*, 371−376.
(6) van der Mei, H. C.; Bos, R.; Busscher, H. J. *Colloids Surf. B, Biointerfaces* **1998**, *11*, 213−221.
(7) Partensky, F.; Hess, W. R.; Vaulot, D. *Microbiol. Mol. Biol. Rev.* **1999**, *63*, 106−127.
(8) Legendre, L.; Demers, S.; Delesalle, B.; Harnois, C. *Marine Ecol.−Prog. Ser.* **1988**, *47*, 153−160.
(9) Zubkov, M. V.; Sleigh, M. A.; Burkill, P. H. *Aquatic Microbiol. Ecol.* **2000**, *21*, 13−20.
(10) Saito, M. A.; Rocap, G.; Moffett, J. W. *Limnol. Oceanogr.* **2005**, *50*, 279−290.
(11) Stockner, J.; Callieri, C.; Cronberg, G. In *The Ecology of Cyanobakteria*; Whitton, B. A., Potts, M., Eds.; Kluwer Academic Publishers: Amsterdam, The Netherlands, 2000; pp 195−231.
(12) Dittrich, M.; Kurz, P.; Wehrli, B. *Geomicrobiology* **2004**, *21*, 45−53.
(13) Thompson, J. B.; Schultze-Lam, S.; Beveridge, T. J.; Des Marais, D. *Limnol. Oceanogr.* **1998**, *42*, 133−141.
(14) Obst, M.; Dittrcih, M. *Geobiology* **2005**, *3*, 179−193.
(15) Benning, L. G.; Phoenix, V. R.; Yee, N.; Tobin, M. J. *Geochim. Cosmochim. Acta* **2004**, *68*, 729−741.
(16) Fowle, D. A.; Fein, J. B. *Chem. Geol.* **2000**, *168*, 27−36.
(17) Fein, J. B., Daughney, C. J., Yee, N., Davis, T. A. *Geochim. Cosmochim. Acta* **1997**, *61*, 3319−3328.
(18) Wei, J.; Saxena, A.; Song, B.; Ward, B. B.; Beveridge, T. J.; Myneni, S. C. B. *Langmuir* **2004**, *20*, 11433−11442.
(19) Sokolov, I.; Smith, D. S.; Henderson, G. S.; Gorby, Y. A.; Ferris, F. G. *Environ. Sci. Technol.* **2001**, *35*, 341−347.
(20) Obst, M.; Dittrich, M.; Kuehn, H. *G*^{3} **2005**, submitted.
(21) Naumann, D.; Schultz, C.; Helm, D. In *Infrared Spectroscopy of Biomolecules*; Mantsch, H. H., Chapman, D., Eds.; Wiley-Liss, Inc.: New York, 1996; pp 279−310.
(22) Kansiz, M.; Heraud, P.; Wood, B.; Burden, F.; Beardall, J.; McNaughton, D. *Phytochemistry* **1999**, *52*, 407−417.
(23) Omoike, A.; Chorover, J.; Kwon, K. D.; Kubicki, J. D. *Langmuir* **2004**, *20*, 11108−11114.
(24) Parikh, S. J.; Chorover, J. *Geomicrobiol. J.* **2005**, *22*, 207−218.

10.1021/la0531143 CCC: $33.50
Published on Web 05/10/2006

functional groups of two wild cyanobacteria strains and showed that their pK_a and concentrations are similar to that of Gram-positive bacteria.[25] Nevertheless, the influence of pH and Ca concentration on the cell surface and the structure of surface functional groups of the *Synechococcus* strain PCC 7942, which is a very well investigated strain from physiological and biochemical points of view,[26−28] remains unclear.

The objective of our research was to obtain specific information on functional groups in aqueous bacterial suspensions and to evaluate their variation as a function of pH and dissolved Ca concentrations. By modeling the experimental results, we expect to obtain the complexation constants and gain insight into the mechanisms of Ca adsorption on bacterial cells. Potentiometric titrations were used to identify major proton-active functional groups and surface charges over the pH range of 4−10. Attenuated total reflectance Fourier transform infrared (ATR-FTIR) spectroscopy was used to examine the interfacial properties of the cells. Here we present the pK_a's and concentrations of binding sites of *Synechococcus* PCC 7942, their molecular characteristics, and dependence on pH and calcium concentrations.

2. Methods

2.1. Picocyanobacteria Growth. In all of the experiments presented here, the freshwater cyanobacteria *Synechococcus* PCC 7942 strain was obtained from the Pasteur Institute (Paris, France). Cells were grown as a batch culture using modified Z/10 medium (5.9 mg L^{-1} $Ca(NO_3)_2 \cdot 4H_2O$, 46.7 mg L^{-1} $NaNO_3$, 4.1 mg L^{-1} $K_2HPO_4 \cdot 3H_2O$, 2.5 mg L^{-1} $MgSO_4 \cdot 7H_2O$, 168 mg L^{-1} $NaHCO_3$, 11.45 mg L^{-1} Na-EDTA, 3 mg L^{-1} $FeSO_4 \cdot 7H_2O$, 248 μg L^{-1} H_3BO_3, 135 μg L^{-1} $MnSO_4 \cdot H_2O$, 7.2 μg L^{-1} $(NH_4)_6 \cdot Mo_7O_{24} \cdot 4H_2O$, 23.2 μg L^{-1} $ZnSO_4 \cdot 7H_2O$, 12 μg L^{-1} $Co(NO_3)_2 \cdot 6H_2O$, 10.4 μg L^{-1} $CuSO_4 \cdot 5H_2O$) under a 14 h/10 h light/dark condition, with a light intensity of approximately 10 μE m^{-2} s^{-1}. Cells in the stationary growth phase were used for the titration experiments. Cell viability was verified using epifluorescence microscopy.

2.2. Preparation of Cells. The cultures were harvested by centrifugation at 7000 rpm for 10 min at 20 °C. The medium was decanted and the cells were re-suspended in 0.001M EDTA. After further centrifugation at 7000 rpm for 10 min, the EDTA solution was decanted; the cells were re-suspended in 0.1 M $NaNO_3$ and centrifuged under the same conditions as above. The washing procedure in $NaNO_3$ was repeated four times, and the cells were finally batched and re-suspended in 5 or 10 mL of 0.1 M $NaNO_3$.

2.3. Potentiometric Titration. *Solutions.* All solutions were prepared through analytical measurements to determine molar concentrations. The solutions were subsequently degassed with N_2 for 20 min to dissipate O_2 and CO_2. Approximately 0.1 M NaOH solution was prepared from NaOH using degassed 18 MΩ water. The exact NaOH concentration was determined prior to the titration experiment through the titration of three 5 or 10 mL aliquots with standard 0.1 M HCl. The three runs had a relatively standard deviation of 1%.

Titrator Setting. Deprotonation constants and surface site concentrations were determined from acid−base titrations of bacterial suspensions in a background electrolyte of 0.1 M $NaNO_3$. All titrations were performed in a glass vessel with a lid as part of a Metrohm GP 736 Titrino unit interfaced by Titrino software TITRINET to a personal computer. Two separate buret exchange units with 20 and 10 mL were used, one for the acid and one for the base. We also used a Metrohm titrator vessel lid. The temperature was recorded with a temperature sensor; the error of the temperature probe was 0.1 °C. The pH electrode was three-point calibrated with buffers (pH 4, 7, and 10) before each experiment, and the slope did not deviate more than 1% from the Nernst value.

The Titrino unit was programmed with a dynamic mode for the titration, which adds the variable amount of titration solution according to the pH changes: the smaller volume of solution was added at the slope of the pH curve. The successive titrant additions were made only when the signal drift reached 10 mV min^{-1}

Bacteria Titration. The titrator electrode was first calibrated as mentioned above. The optical density (OD 630 nm) of the bacterial suspension in the $NaNO_3$ electrolyte solution was measured prior to each titration run. The measured absorbance was compared to a prepared calibration curve to determine the concentration of bacteria (in mg L^{-1}) and the bacterial cell numbers (cells L^{-1}). The dry weight of bacteria was defined by drying at 65 °C until a constant weight was attained. The absorbance used was in the range of 0.41−0.81, which corresponds to 0.063−0.122 g of bacteria L^{-1}. A known amount of bacterial suspension, approximately 50 mL, was then transferred to the titration vessel, which was immediately attached to the lid setup connected with the N_2 gas line. A magnetic stir bar was also added to the vessel. The whole system was then degassed for 30−40 min to exclude atmospheric CO_2. Following the degassing procedure, a positive pressure of N_2 was maintained by allowing a gentle flow of N_2 into the headspace during the titration.

The bacterial aliquot was then titrated quickly to pH = 2.9 with 0.1 M HCl. The buret unit was subsequently changed, and the titration of the aliquot with NaOH up to pH = 10 began. The total time for each titration was approximately 40 min.

Some titrations were reversed by conducting an acid titration, which immediately followed the base titration. The results of the reversed titrations were not significantly different to the forward titrations suggesting reversibility of the proton adsorption−desorption reactions.

2.4. Attenuated Total Reflectance Infrared (ATR−IR) Spectroscopy. ATR−IR measurements were performed on a Bio-Rad FTS 45 Fourier transformation infrared (FTIR) spectrophotometer with a 32000 data station. Scans (n = 256) with 1 cm^{-1} resolution were collected for each suspension spectrum of washed bacteria in 0.1 M $NaNO_3$. The suspension (~0.5 g L^{-1}) was left to settle for 1−2 h; the spectra were then measured. The spectrum of 0.1 M $NaNO_3$ was used as a background. The baseline shift of the spectra was corrected using the MATLAB application (The Math Works, Inc., Natrick, MA).

To study the influence of pH and Ca concentrations on the binding sites of cells, bacteria solutions of defined pH and Ca concentrations were allowed to settle over 1−2 h and spectra were acquired. $CaCl_2$ solution was added to the washed cell suspension resulting in calcium concentrations ranging from 0 to 2.5 mM with pH = 6.64 and pH values varying from 3.03 to 8.84. The spectrum of a electrolyte was used as a background.

The penetration depth of the IR radiation into the sample depends directly on the wavelength, but it is also affected by other parameters of the system given in the following equation.[29] *Penetration depth* is defined as the depth at which the intensity of the evanescent wave has dropped to 1/e of its value at the surface.

$$\text{penetration depth} = \frac{\lambda}{2\pi(n_p^2 \sin^2\theta - n_s^2)^{1/2}} \qquad (1)$$

Here λ is the wavelength (cm^{-1}), θ stands for the angle of internal reflection, n_p denotes the refractive index (RI) of the crystal, and n_s refers to the refractive index of the sample. For a diamond (RI = 2.4) with an incident angle of 50° and assuming it has an RI of approximately 1.39 for bacterial cell material, the depth penetration is calculated to be about 0.735 μm at 1800 cm^{-1} and about 1.3 μm at 1000 cm^{-1}. Given that the studied strain PCC 7942 had elongated shapes with a diameter of 0.5 μm and a length of 2.3 μm and that cells are likely to accumulate onto the surface of the IRE, it is possible that ATR measurement reveals at least one layer of the

(25) Dittrich, M.; Sibler, S. *J. Colloid Interface Sci.* **2005**, *286*, 487−495.
(26) Porta, D.; Bullerjahn, G. S.; Durham, K. A.; Wilhelm, S. W.; Twiss, M. R.; McKay, R. M. L. *J. Phycol.* **2003**, *39*, 64−73.
(27) Miyachi, S.; Iwasaki, I.; Shiraiwa, Y. *Photosynth. Res.* **2003**, *77*, 139−153.
(28) Erez, J. B.; Kaplan, A. *Can. J. Bot.* **1998**, *76*, 1109−1118.
(29) Harrick, N. J. *Internal reflection spectroscopy*; Interscience Publishers: New York, 1967.

whole cell and possibly several layers in parts of the spectrum. Our TEM investigations showed that the membrane of PCC 7942 was about 20 nm.[20] Hence, the ATR-FTIR spectrum of individual bacteria reflects the sum of the molecular structures of the whole organism, including cell walls and membranes and the internal structures.

An ATR crystal with higher refractive indices (e.g., a Ge ATR crystal with RI = 4) and which is accepting an infrared beam at 60° incident angles will give a shallower penetration depth (around 500 nm for 100 cm^{-1} and 280 nm at 1800 cm^{-1}). On the basis of our calculations, it is apparent that the beam will penetrate the interior of the bacterial cells, which are attached to the ATR crystal surface. The calculation of penetration depths includes some uncertainties. First, during the measurements, some cells are in contact with the crystal and some are separated from the crystal by an intermediate water film. The latter has an unknown thickness and a lower refractive index compared to the cells. Therefore the calculated penetration depth is valid only for the attached cells. Moreover, the refractive indices of bacterial cell walls which strongly alter penetration depth are difficult to estimate, because of its macromolecular structure and its variation with solution composition. Hence, ATR-FTIR spectra of bacteria suspension cannot be attributed to the surfaces alone.

However, recent experimental studies demonstrated that ATR-FTIR spectra of bacterial suspensions are likely to reflect the characteristics of functional groups of cell walls. Wei et al. have recently shown that ATR-FTIR spectra of bacterial suspensions are highly sensitive to surfaces. Penetration depths in their experiments were 339 nm at 1000 cm^{-1} and 188 nm at 1800 cm^{-1} which are definitely higher than the average thickness of the bacterial cell wall (ranges from 20 to 50 nm).[18] They were able to demonstrate that ATR-FTIR spectra of a bacteria suspension mostly reflect the properties of the bacterial cell wall and not the interior of the cell.

2.5. Data Analysis. The titration data were analyzed using the linear programming method (LPM) or so-called pK_a spectrum method as proposed by Brassard[30] and applied for bacteria suspension by Cox and Sokolov.[19,31] Proton dissociation from cell surface ligands can be described by the following equation:

$$HL^0 \leftrightarrow H^+ + L^- \tag{2}$$

where L^- is the proton binding site on the cell and H^+ is a proton in solution. The concentration of protonated and deprotonated surface sites can be quantified with the corresponding mass action equation

$$K_a = \frac{[H^+][L^-]}{[HL^0]} \tag{3}$$

where K_a is the acidity constant.

Therefore, for the *j*th addition of acid or base, the charge balance expression can be written[30]

$$C_{Bj} - C_{Aj} + [H^+]_j - [OH^-]_j = \sum_{i=1}^{n}\left(\frac{K_{a_i}L_{T_i}}{K_{a_i} + [H^+]_j}\right) + S \tag{4}$$

where C_{Bj} and C_{Aj} correspond to concentrations of base and acid for the *j*th addition of titrant, $[H^+]_j$ and $[OH^-]_j$ are obtained from the measured proton concentration, and *S* is a constant term analogous to the acid neutralizing capacity or the initial protonation state of the surface.[30,32] The surface sites are considered as a sum of *n* monoprotonic ligands $[L^-]$ with dissociation constants K_{ai} and total concentrations L_{Ti}. In practice, *S* allows a modeling positive charge on the surface. Representing the titration curve as a sum of monoprotonic sites can only account for negative charge using $[L^-]$ terms. The terms on the left can be estimated using experimental data, and the terms on the right are the fitting parameters.

Equation 4 could be solved by fixing the pK_a values as a grid from a minimum to maximum value at fixed step sizes.[31] The ligand concentration associated with each pK_a value is assigned a positive value where zero is a possible result; the result is the so-called pK_a spectrum. The pK_a spectrum approach is used here to determine the best fit of K_{ai}/L_{Ti} pairs, with pK_a values fixed as a grid from 4 to 10 at fixed step sizes (0.2). Once the pK_a values are selected, the matrix version of eq 4 is set up as $Ax = b$. The entry α_{ij} in the $m \times n$ matrix *A* for *n* proposed sites and *m* additions of titrant is

$$\alpha_{ij} = \frac{K_{a_i}}{K_{a_i} + [H^+]_j} \tag{5}$$

The $n \times 1$ vector *x* contains the ligand concentrations for each of the *m* sites and the $m \times 1$ vector *b* contains the measured charge excess $C_{Bj} - C_{Aj} + [H^+]_j - [OH^-]_j$. The matrixes used to solve the linear programming problem were setup as in Brassard[30] and solved using the MATLAB application linear programming routine (http://info.wlu.ca/~wwwchem/faculty/Smith/Research/research.shtml).

2.6. Biosorption Trials. The specific uptake of Ca at different equilibrium pH's was determined by using an experimental procedure described by Pagnanelli[33] as "subsequent additions method" (SAM): about 2−3 g L^{-1} bacterial biomass was washed by the same procedure as that for titration experiments. The first addition of a concentrated solution of $CaCl_2$ (5 mM) was injected to the cellular suspension maintained in agitation, the pH was adjusted and the first sample of 2 mL was taken. After 60 min, the system reaches equilibrium and 2 mL of the suspension was taken, centrifuged, and later analyzed by an inductively coupled plasma-optical emission spectrometer (ICP−OES) to determine the residual calcium concentration. A second addition of the concentrate $CaCl_2$ was made, the pH was measured and adjusted if necessary, and the previous procedure was repeated.

The SAM procedure was repeated using samples without biomass but still making the same additions and drawings: these blank samples are necessary to avoid confusion between the biosorption uptake and the possible precipitation. The evaluation of the metal specific uptake *q* (mmol g^{-1} of bacteria) is obtained by using the mass balance of the metallic ion in the system.

3. Results and Discussion

3.1. pH Influence on Functional Groups: Infrared Spectroscopy Studies. The infrared spectra of *Synechococcus* PCC 7942 in aqueous solution as a function of pH were examined using ATR−IR spectroscopy (Figure 1). Their infrared spectra exhibit distinct peaks corresponding to carboxyl, amide, phosphate, and carbohydrate groups (Table 1).

3.1.1. Carboxylic Groups. Spectra of *Synechococcus* PCC 7942 suspended in 0.1 M $NaNO_3$ over the pH range 3.03−8.24 indicate progressive H^+ dissociation of carboxylic groups (Figure 1). The carboxylic groups of bacterial cells exhibit a distinct band at ~1720 cm^{-1} corresponding to the C═O in acidic cell suspension (pH ≤ 4). The intensity of this peak decreased as the sample pH increased from 3.03 to 4.32 and disappeared at pH = 5.89. This spectral change was similar to that observed by Wei[18] of glucuronic acid and of free EPS.[34]

At a pH range of over 3.03, a new band corresponding to symmetric stretching of carboxylate (−COO−) anion emerges at 1388 cm^{-1}. The −COOH bonds of carboxylic acids absorb in the energy region of 1240 cm^{-1}, the signal was present in acid suspension and was absent at pH ≥ 5.82. Our results suggest that protons can rapidly protonate carboxylic groups of bacterial cells.

(30) Brassard, P.; Kramer, J. R.; Collins, P. V. *Environ. Sci. Technol.* **1990**, *24*, 195−2001.
(31) Cox, J. S.; Smith, D. S.; Warren, L. A.; Ferris, F. G. *Environ. Sci. Technol.* **1999**, *33*, 4514−5421.
(32) Cernik, M.; Borkovec, M.; Westall, J. C. *Environ. Sci. Technol.* **1995**, *29*, 413−425.
(33) Pagnanelli, F.; Papini, M. P.; Toro, L.; Trifoni, M.; Veglio, F. *Environ. Sci. Technol.* **2000**, *34*, 2773−2778.
(34) Omoike, A.; Chorover, J. *Biomacromolecules* **2004**, *5*, 1219−1230.

Table 1. Absorption Bands of Bacterial Surface Functional Groups

wavenumber, cm^{-1}	assignment	comments
~1740	νC═O of ester functional groups primarily from membrane lipids and fatty acids[52]	
~1650	νC═O of amides associated with proteins[53,54]	usually called the amide I band
~1540	δN−H and C−N stretching of amides associated with proteins[53,54]	usually called the amide II band, may also contain contributions from C═N stretches
~1455	CH_3 scissoring, $\delta_{ac}CH_2/\delta_{ac}CH_3$ of proteins[55]	the positions of these broad peaks vary in the literature, called the amine III band
~1398	$\delta_{ac}CH_2/\delta_{ac}CH_3$ and $\nu_s COO^-$ of carboxylic groups[53,55]	the positions of these assignments vary in the literature
~1240	ν_{as}P═O of the phosphodiester backbone of nucleic acid (DNA and RNA) and COOH	general phosphoryl groups
~1200−900	νC−O−C of polysaccharides[55,56], ~1165, ~1110, 1050, 1030 for C−O, -$P(OH)_2$, ~1085, stretching of P═O in phosphate ~1211	the predominant polysaccharide in cyanobacteria is glycogen
~ 1080	ν_sP═O of the phosphodiester backbone of nucleic acid (DNA and RNA)[53,56]	may also be due to the presence of phosphorylated proteins and polyphosphate storage products
~950−1150	asymmetric and symmetric stretching of PO_2^- and $P(OH)_2$ in phosphate; vibrations of C−OH and C−C bonds in polysaccharides and alcohols.	

3.1.2. Amide Groups. The amide groups exhibit intense bands at around 1650 and 1550 cm^{-1} corresponding to the amide I and II, respectively. Although variations in the energy of these bands were minor with changes in pH, the intensity ratio of amide band I to II increased with an increase of pH. Over the pH range 3.02−8.24, the amide I band shifts from 1652 to 1649 cm^{-1} and amide II from 1543 to 1546 cm^{-1}.

The minor variations in the infrared spectra of amide groups may be caused first by the appearance of new peaks in this energy region (e.g., corresponding to COO^- 1590 cm^{-1}) and second by changes in protein conformations. According to the titration experiments, functional groups (see section 3.2) on the surface *Synechococcus* PCC 7942 have pK_a's at 9.1 and 10. As a result, the insensitivity of amide vibrations may be caused by lower pH values in the range of 3.03−8.24 in the infrared experiments.

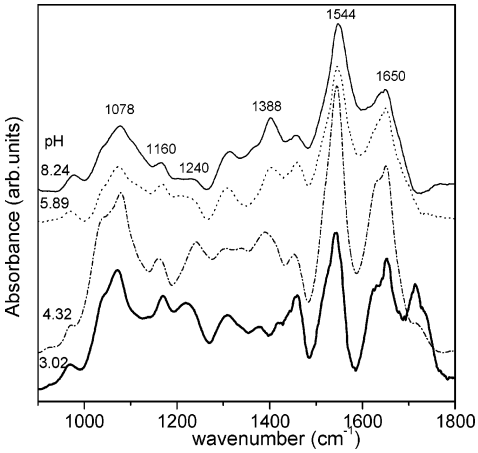

Figure 1. ATR−FTIR spectra of intact cells of *Synechococcus* PCC 7942. Spectra were collected for cells at different pH values (thick line indicates pH = 3.03, dash dot line indicates pH = 4.32, dot line indicates pH = 5.89 and solid line indicates pH = 8.24). Approximate band positions are indicated in the figure. See Table 1 for specific band assignments.

3.1.3. Phosphate Groups. Phosphate groups in bacteria can exist in several different forms: inorganic forms of phosphate such as orthophosphate and its oligomers, and organic species in the form of phosphate mono- and diesters.

Upon protonation of aqueous inorganic phosphates, the asymmetric stretching vibration shifted to an energy level of 1077 (HPO_4^{2-}), 1155 ($H_2PO_4^-$), and 1174 cm^{-1} ($H_3PO_4^0$).[35] We observed in experiments that the band around 1078 cm^{-1} was not strongly affected by pH variations. This fact may be caused by the occurrence of functional groups such as phosphate groups inside the cell wall.

Phosphate oligomers also exhibit features similar to those of protonated phosphates. The asymmetric stretching modes of the PO_4 in unprotonated groups were in the range between 1160 and 1240 cm^{-1}.[18] It therefore remains difficult to unambiguously identify different phosphate groups from the infrared spectra alone. With deprotonation, the bands decreased in intensity and shifted to lower energy, where bands can overlap with carboxyl groups. We observed peaks at 1170 cm^{-1} which decreased with an increase of pH, shifted to lower energy, and were almost absent at pH = 8.24. These spectral changes may be caused by a deprotonation of phosphate groups with pK_a's = 6.88 of titration experiments (see 3.2). These observations are supported by ATR-FTIR spectra of modeled molecules of carboxylic acid and phosphate groups where the pH dependent spectral variations around 1200 cm^{-1} have been attributed to phosphate groups.[18]

3.1.4. Polysaccharide and Related Groups. The C−OH groups, C−C, and some of the C−H vibrations exhibited a broad band in the energy region of 950−1150 cm^{-1}. With an increase in pH, the line width of the band at 1078 cm^{-1} decreased along with the decrease in the intensity of a weak band around 1050 cm^{-1}.

(35) Persson, P.; Nilsson, N.; Sjorberg, S. *J. Colloid Interface Sci.* **1996**, *177*, 263−275.

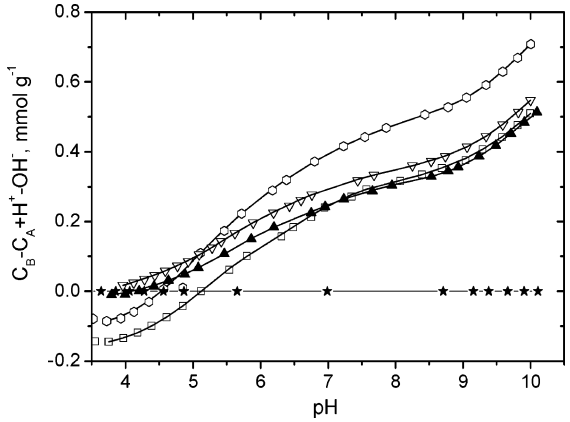

Figure 2. Acid/base titration data from the titration performed using *Synechococcus* PCC 7942. Also shown is the titration curve for the electrolyte in the absence of bacteria (star symbols). H^+ exchanged for replicate acid−base titrations from the same population (0.6 g L^{-1}) in 0.1 M $NaNO_3$. Closed symbols correspond to the forward titration data, and open symbols correspond to the back-titration. Lines correspond to the calculations by liner programming.

These changes were maximal between pH 3.03 and 4.32 and may be caused by variations in the H-bonding interactions associated with the deprotonation of carboxylate groups and the variations in the protonation state of the phosphate group.

A strong band at 1450 cm^{-1} was insensitive to pH variation, and this is characteristic of the scissoring motion of CH_2 groups,[36] which are common in peptidoglycan, teichonic acids, LPS, and phospholipids. Wei et al.[18] also observed similar peaks in ATR-FTIR spectra of the Gram-positive and Gram-negative bacteria.

3.2. Potentiomentric Titrations. Figure 2 shows the titration curves for *Synechococcus* PCC 7942 cells following the transformation to the charge balance expression of four replicate titrations. Consistent trends are observed for the titration curves in each set. These results demonstrate that reproducible quantitative titration curves can be obtained for estimates of surface characteristics, although some surface variability may occur with the same bacterial strain. The comparison of the titration with the electrolyte clearly shows that the presence of bacteria influences the buffering capacity of the electrolyte. However, the bacterial suspension displays relatively weak inflection points. This behavior has been attributed to the existence of several functional groups with similar p*K* values.[37]

The results of the titration experiments were used to generate a description of the number of concentrations and thermodynamic properties of ionisable functional groups on the bacterial surface.

The specific adsorption of electrolyte ions onto the bacterial surface was not considered as it would require titration experiments over a range of several orders of magnitude with respect to electrolyte concentration. The bacterial surface however reacts sensitively to extreme shifts of salinity: cells may undergo spontaneous lysis in solutions with low ionic strength, and the membrane-bound proteins tend to solubilize at significantly higher ionic strength.[31,38] The ability of cells of *Synechococcus* PCC 7942 to undergo osmotic volume adjustments was irreversibly impaired when they were exposed to 0.5 M NaCl.[39]

3.3. Functional Groups on the Cell Surface. The pK_a spectra resulting from fitting the data from replicate titrations using the linear programming method (LPM) are shown in Figure 3. The replicate titrations exhibit some variation in terms of site numbers plus pK_a and L_T values, but the overlay spectrum shows distinct clusters of pK_a values. To summarize these data, five ranges of pK_a values were determined by inspection and assigned to five different classes of ligands (Table 2). Our results allowed the

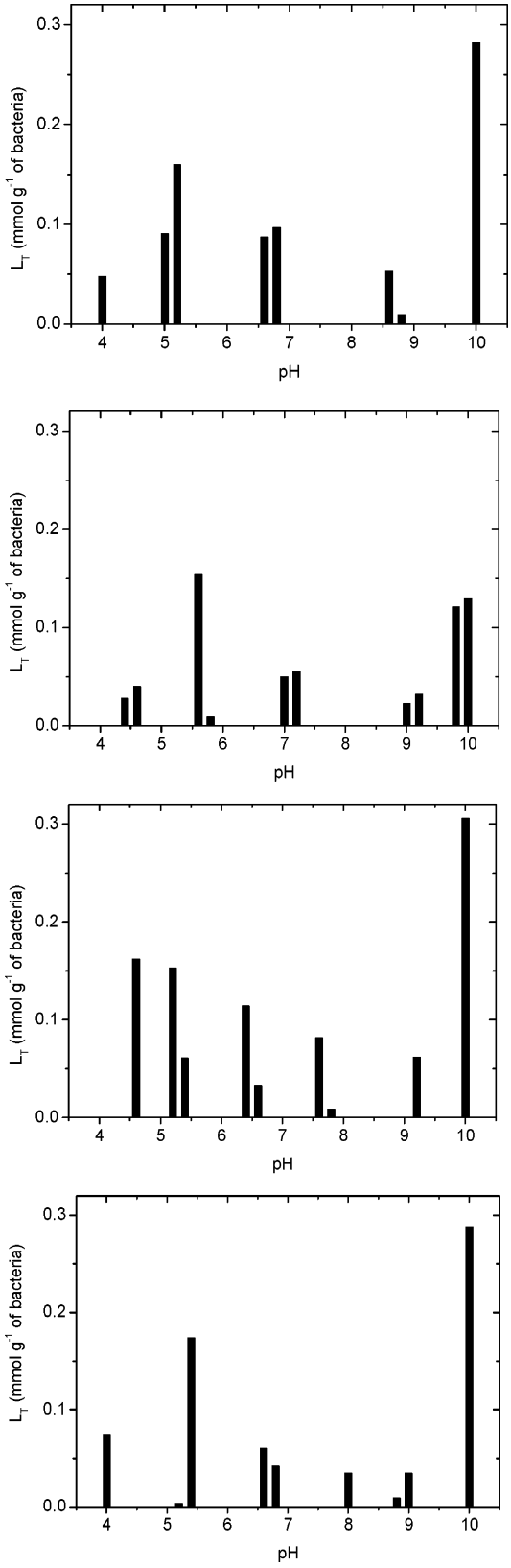

Figure 3. pK_a spectra determined by linear programming analysis for each of the four titration curves shown in Figure 2.

(36) Pourchert, C. J. *The Aldrich Library of FT-IR Spectra*; Aldrich: Milwaukee, WI, 1997.
(37) Seki, H.; Suzuki, A.; Mitsueda, S. *J. Colloid Interface Sci.* **1998**, *197*, 185−190.
(38) Voet, D.; Voet, J. G. *Biochemistry*; Wiley: New York, 1995.
(39) Ladas, N. P.; Papageorgiou, G. C. *Photosynthetica* **2000**, *38*, 343−348.

Table 2. Summary of pK_a Values for Five-Sites Model Obtained from Analysis of *Synechococcus* PCC 7942 Titration Data by Linear Programming

ligand class	range of pK_a	pK_a values	L_T, mmol g^{-1}	functional group
1	4.0−4.6	4.35 ± 0.19	0.063 ± 0.007	carboxylic
2	4.6−5.2	5.24 ± 0.13	0.210 ± 0.017	carboxylic
3	6.5−8.0	6.88 ± 0.27	0.168 ± 0.025	phosphoryl
4	8.6−9.2	9.10 ± 0.15	0.056 ± 0.004	amine/hydroxyl
5	9.75−10	10.00 ± 0.01	0.281 ± 0.011	amine/hydroxyl

mean value to be calculated, which was 0.269 ± 0.08 mmol g^{-1}. For each ligand class, a mean pK_a value was determined by using a weighted mean calculation, where the weighting factors were the corresponding ligand concentrations. A confidence region of this estimate was calculated using a weighted standard deviation calculation.[31] The five-site model for *Synechococcus* PCC 7942 is summarized in Table 2.

Pagnanelli et al.[33] identified two groups on the surface of *Arthrobacter* sp. (pK_1 = 6.9 and pK_2 = 10.1), which they assigned to phosphoryl and amine groups. To describe the proton binding of Gram-negative *S.putrefaciens*, Sokolov et al.[19] also proposed a five-sites model with the acidic sites attributed to phosphodiester sites (pK_a = 3.72 ± 0.06) and carboxylic/phosphodiester sites (pK_a = 4.95 ± 0.02), intermediate sites corresponding to phosphoryl sites (pK_a = 6.64), and the highest pK_a sites attributed to amine (pK_a = 8.83 ± 0.02) and amine/hydroxyl sites (pK_a = 9.99 ± 0.01). Conversely, Cox et al.[31] suggested that two of their distinct sites could be of the same functional group, which they assigned to carboxyl moieties. The pK_a value of the most acidic *Synechoccoccus* PCC 7042 site is intermediate between those proposed by Cox et al. and Sokolov et al.[19,31] The acidic (4.3) and intermediate (6.88) pK_a values are similar to the pK_a from other cyanobacteria strains[25] and a Gram-negative strain.[40]

The titration data does not provide clear evidence for an assignment of the acidic groups with pK_1 = 4.35 and 5.24 to carboxyl groups (pK_a = 2−6). However, the spectral observations of the band at 1170 cm^{-1} in the ATR-FTIR experiments (see section 3.1) supported the interpretation of deprotonating carboxyl groups with a pK_a = 4.14 obtained from the modeling of potentiometric titrations (see section 3.2). Furthermore, the disappearance of the −COOH bonds of carboxylic acids in the energy of 1720 cm^{-1} at pH > 5.82 is consistent with the second carboxylic pK_a value of 5.24 calculated from the titration experiments.

The decrease of the spectral peak at 1170 cm^{-1} with an increase of pH and its almost absence at pH = 8.24 are consistent with the existence of a phosphate group with pK_a = 6.88. The spectral experiments showed the insensitivity of amide vibrations around 1650 and 1550 cm^{-1} by lower pH values in the range of 3.03−8.24. This result may be caused by functional groups attributed to amine/hydroxyl groups with pK_a's at 9.1 and 10.

By combining the ATR-FTIR data, the pK_a values in the *Synechococcus* PCC 7942 strain from titration experiments, and pK_a values determined in previous studies,[41,25,31] we can assign sites with pK_a = 4.35 and 5.24 to carboxyl (pK_a = 2−6), pK_2 = 6.88 to phosphoryl (pK_a = 5.6−7.2), and the remaining values of pK_a = 9.1 and 10.0 to amine (pK_a = 9.0−11.0) and hydroxyl (pK_a = 8−12) groups.

The total concentration of functional groups of *Synechococcus* PCC 7942 0.78 mmol g^{-1} is slightly lower than values determined for other cyanobacterial strains 1.77[19] and 1.27 mmol g^{-1}.[40] The total concentration of functional groups of cyanobacterial strains appears to be similar to that of Gram-positive bacteria despite differences in structures of the cell walls.[40,41] The cell walls of Gram-positive bacteria are characterized by a thick external layer surrounded by a cell envelope of peptidoglycan (PG). The PG layer of Gram-negative bacteria is much thinner than what is typical for Gram-positive bacteria and is surrounded by an outer membrane. It is possible that the liposaccharides, which are the major part of an outer membrane, are partly responsible for the buffering capacity.

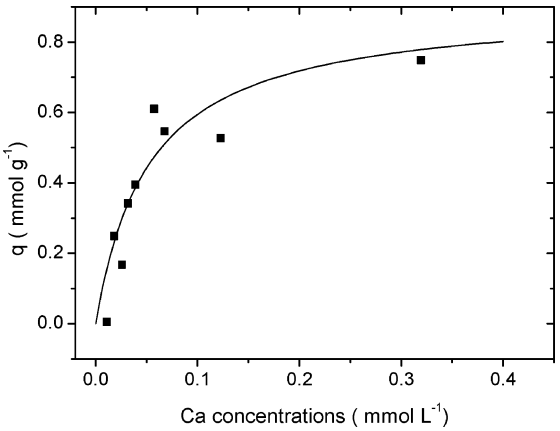

Figure 4. Biosorption data on Ca uptake by *Synechococcus* PCC 7942 suspension. Symbols are experimental data and solid line is the respective Langmuir isotherm.

Table 3. Langmuir Parameters Obtained from Ca Biosorption Data at pH = 7 and Ca Binding Constants

q_i, mmol g^{-1}	b_i, L mmol^{-1}	pK_{Mi}
0.283	19.067	4.1
0.380	19.056	4.0
0.244	19.06	5.4

3.4. Sorption Isotherm of Calcium. As calcium is known to be an important competitor for metal ion sorption, it is important to be able to calculate the calcium binding at different pH concentrations. The Langmuir sorption model was used for experimental data fitting (eq 6) where q_{max} (mmol g^{-1} of biomass) is the maximum specific calcium uptake and b (L mmol^{-1}) is the ratio of the adsorption/desorption rates.

$$q = \frac{q_{max} b C_{eq}}{1 + b C_{eq}} \quad (6)$$

Figure 4 reports the experimental data of Ca biosorption and the respective Langmuir isotherms at equilibrium pH = 7. For experimental data fitting, the parameters were estimated by using the Levenberg−Marquard method.[42,43] Langmuir isotherm characteristic parameters and calcium binding constants are shown in Table 3. Supposing that every site reacts only according to one mechanism, an adequate set of reactions to describe Ca data was suggested. Ca ions are supposed to react with two carboxylic and one phosphate groups, where their sites concentrations and equilibrium constants are those determined in the titration curve modeling according to the results of ATR-FTIR and titration experiments (Table 2).

(40) Ngwenya, B. T.; Sutherland, I. W.; Kennedy, L. *Appl. Geochem.* **2003**, *18*, 527−538.
(41) Yee, N.; Benning, L. G.; Phoenix, V. R.; Ferris, F. G. *Environ. Sci. Technol.* **2004**, *38*, 775−782.
(42) Levenberg, K. *Q. Appl. Math.* **1944**, *2*, 164−168.
(43) Marquardt, D. W. *SIAM J. Appl. Math.* **1963**, *11*, 431−441.

$$S_1H \leftrightarrow S_1^- + H^+, K_{a1} = \frac{[S_1^-][H^+]}{[S_1H]} \quad (7)$$

$$S_2H \leftrightarrow S_2^- + H^+, K_{a2} = \frac{[S_2^-][H^+]}{[S_2H]} \quad (8)$$

$$S_3H \leftrightarrow S_3^- + H^+, K_{a3} = \frac{[S_3^-][H^+]}{[S_3H]} \quad (9)$$

$$S_iH + Ca^{2+} + OH^- \leftrightarrow S_iHCa(OH)^+, K_{Mi} = \frac{[S_iHCa(OH)^+]}{[S_iH][Ca^{2+}][OH^-]} \quad (10)$$

where $i = 1-3$ and K_{M1}, K_{M2}, and K_{M3} are the formation constants of the three hypothesized systems $S_iHCa(OH)^+$. Although bioaccumulation (metabolism dependent mechanism) may take place, this phenomenon was considered negligible.

Combining the equilibrium constants (eqs 7−10) and the site mass balance (eq 11) reported below, it is possible to obtain eq 12 for the total specific uptake (mmol g^{-1})

$$[S_i]_{tot} = [S_i^-] + [S_iH] + [S_iHCa(OH)^+] \quad (11)$$

$$q = \sum_{i=1-3}\left(\frac{[S_i^-]_{tot}K_{Mi}K_W[Ca^{2+}]}{[H^+] + K_{ai} + K_{Mi}K_W[Ca^{2+}]}\right) \quad (12)$$

where K_{M1}, K_{M2}, and K_{M3} are the formation constants of the three hypothesized systems $S_iHCa(OH)^+$.

The first binding constants are higher than those that has been recently reported for Ca complexation reactions on cell surfaces of Gram-positive *Bacillus* cells 2.7 and 2.5.[44] Gorman−Lewis results revealed that uranyl can form stable surface complexes on bacterial cell walls in the presence of calcium.[44] Therefore, the stability constants of the metal−bacterial surface complexes will help us to estimate the potential impact of bacterial surface adsorption on the mobility of metal.

The ionic strength was not maintained as constant during the biosorption experiments. Despite the large number of proposed thermodynamic models and electrostatic treatments, very few studies have examined the effect of ionic strength on bacteria adsorption reactions over a broad range of electrolyte concentrations. In the presented biosorption experiments, the ionic strength changed from 1.25×10^{-4} to 1×10^{-3} M. Proton binding depends on ionic strength, and the simplest way to analyze the electrostatic effects is to analyze experimental data using a model with additional terms describing these effects. Recently the effect of a broad range of ionic strength (0.001−0.6 M) on apparent proton, Cd, and Pb binding constants and apparent site densities for bacterial surfaces was investigated using both nonelectrostatic and electrostatic (diffusive layer and triple-layer treatments) approaches.[45] Results of this study demonstrated that the effect of ionic strength was small. Also Cox et al. using a pK_a-spectra modeling approach for titration experiments at 0.025 and 0.1 M ionic strength showed that, although pK_a values shift in response to the change of ionic strength, the total concentration of proton binding sites available does not dramatically change.[31] This is also assumed in surface complexation models where electrostatic terms modify the pK_a values and not the ligand concentrations.[46,47] Specifically bound protons and calcium compete for the same binding sites on the cell surface. By combining the results of experiments on pH influence with Ca titration experiments, tentative mechanisms of how the calcium binds to the cell at different pH may be drawn. First of all, types of sites that are involved can be defined. Results from the potentiometric titrations and IR experiments with different pHs indicate the presence of strong chemical heterogeneity, which was also observed by atomic force microscopy and chemical scanning microscopy.[18−20]

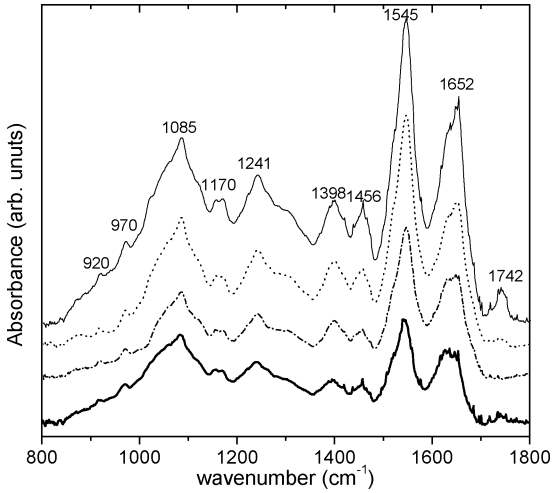

Figure 5. ATR−FTIR spectra of intact cells of *Synechococcus* PCC 7942. Spectra were collected for cells at different Ca concentration values (the thick line indicates a Ca concentration of 0 mM, the dashed−dotted line indicates 0.025 mM, the dotted line indicates 0.25 mM, and the solid line indicates 2.5 mM). Approximate band positions are indicated in the figure.

3.5. Ca Influence on Bacterial Functional Groups: Infrared Spectroscopy Studies. Previous research has shown that adsorption of Ca on the outer membrane of *Synechococcus* PCC 7942 is a very fast (within seconds) process.[20] At acidic pH values, the generation of a large interior-alkaline pH difference between intercellular and external pH seems to be necessary for acid tolerance. Calcium might play a role in the generation of this difference in pH because, in the absence of this cation, cyanobacteria maintained a much smaller pH gradient in acidic solutions.[48] Giraldez-Riez et al. showed that calcium alleviates the acidic sensitivity and so plays an active role directly involved in pH homeostasis of cyanobacteria PCC 7120.[49] One possible mechanism is that increased Ca^{2+} might render the membranes impermeable at low pH. Figure 5 displays a series of infrared spectra collected for a suspension of *Synechococcus* PCC 7942 that was titrated with $CaCl_2$. Ca concentrations changed from 0 to 2.5 mM. As the Ca concentration decreases, the peak position moved toward lower energy from 1652 to 1620 cm^{-1}. These spectral changes may be due to deprotonation of C═O in secondary amides (amide I) or to a decrease of the vibration with the decrease of calcium. With an increase of Ca concentration, the peak at 1085 cm^{-1} exhibited a narrower line with a weakening of the shoulder around 1050 cm^{-1}. These changes may be caused by deprotonation of carboxylate and phosphate groups. With an

(44) Gorman-Lewis, D.; Elias, P. E.; Fein, J. B. *Environ. Sci. Technol.* **2005**, *39*, 4906−4912.

(45) Borrok, D. M.; Fein, J. B. *J. Colloid Interface Sci.* **2005**, *286*, 110−126.

(46) Dzombak, D. A.; Morel, F. M. M. *Surface complexation modeling: hydrous ferric oxide*; Wiley-Interscience: New York, 1990.

(47) Stumm, W. *Chemistry of the solid-water interface: processes at the mineral-water and particle−water interface in natural systems*; Wiley-Interscience: New York, 1992.

(48) Giraldez-Ruiz, N.; Mateo, P.; Bonilla, I.; Fernandez-Pinas, F. *New Phytol.* **1997**, *137*, 599−606.

(49) Giraldez-Ruiz, N.; Bonilla, I.; Fernandez-Pinas, F. *New Phytol.* **1999**, *141*, 225−230.

increase of Ca concentration over 0.25 mM, the peak around 1240 cm^{-1} also became sharper. This band can be assigned to asymmetric PO stretching vibrations in phosphate diesters. This concentration value is consistent with findings of Plette et al.,[50] where calcium sorption on the cell wall of Gram-positive soil bacteria has been investigated. The amount of protons released during the calcium titration equals the amount of calcium sorbed for calcium concentrations up to 0.2 mmol L^{-1} at pH = 5. Consequently, the number of positively charged sites increases thus leading to a gradual decrease in the negative charge of the cell wall. The surface charge becomes positive with 0.2 mmol L^{-1} calcium concentrations.

The spectrum of the *Synechococcus* PCC 7942 suspension at 2.5 mmol L^{-1} Ca concentration is characterized by a distinct absorption at 1740 cm^{-1} arising from the asymmetric stretching vibration of ester C═O functional groups primary caused by lipids and fatty acids. Also the IR spectra collected for this sample showed higher peak intensity (1720 cm^{-1}) than those from samples with lower Ca concentrations. Although Ca biosorption reached a plateau around 0.4 mmol L^{-1} (Figure 4), the spectral intensity increased beyond this calcium concentration (Figure 5).

ATR-FTIR spectra of cell suspensions may be affected by Ca addition in different ways. On one hand, calcium affects properties of a double layer of bacterial cells and Ca adsorption onto bacterial cells lead to a variation of the functional group structure. On the other hand, it was shown that calcium ions play a role in adhesion of bacteria and algae to inert surfaces, so the sedimentation behavior of cell suspensions will be affected.[51] Increase of cell sedimentation due to Ca increase may lead to the increase of spectral intensity. To separate these impacts, experiments over a broad range of ionic strengths are needed together with surface complexation modeling of the results assuming a nonelectrostatic or an electrostatic approach.

4. Summary and Conclusions

The results presented in this study showed that the dominant functional groups of the bacterial surface are carboxyl, amide, phosphate, hydroxyl, and carbohydrate related moieties. Modeling results and IR spectra are consistent with the presence of five distinct surface sites on the bacterial surface with pK_a values of 4.35, 5.24, 6.88, 9.1, and 10.00 with a total concentration of 7.78×10^{-4} mol g^{-1}. The carboxylic and phosphate groups together dominate the surface sites with 34% and 22%, respectively, although the amine and hydroxyl groups represent 36% and 7%. Our results on the deprotonation constants for the different sites are consistent with the findings of other studies.

Among different functional groups, we find that carboxylic, phosphate (pK_{a1} = 4.35, pK_{a2} = 5.24, and pK_{a3} = 6.88), and the deprotonation of the first may explain the negative net charge of the bacteria surface in the pH range of 4−9. Although a majority of carboxylic acid groups have pK_a values below 5, the phosphate groups have a wide range of pK_a values, which decrease with phosphate polymerization. A previous study on a model molecule showed that the phosphate mono- and diesters common in bacteria walls also exhibit strong acidic behavior. The absence of changes in amide groups with pH may suggest that the macromolecular structure of the protein backbone may not change significantly with solution pH.

ATR-FTIR spectroscopic results presented here demonstrate that properties of bacterial functional groups change with a change in calcium concentrations in solutions. Because of their sensitivity in the acidic pH range, both carboxylic and phosphate groups can act as metal binding sites below 5. The chemical modeling reported here is able to predict calcium biosorption data. Although the calcium concentration range common for freshwater systems is tested in these investigations, it was important to verify the influence of concentrations in the presence of other ions (e.g., trace and heavy metals and humic acids) and performed further adsorption experiments. This information will be useful in understanding the role of cyanobacteria in aquatic systems.

Acknowledgment. This research has been partially supported with funding from the Swiss Federal Institute of Technology, ETH, Zurich. We would like to thank Stephan Hug for the access to the infrared spectrometer at Eawag, Bernhard Wehrli, and two anonymous reviewers for their constructive comments that helped us clarify our arguments.

LA0531143

(50) Plette, A. C. C.; Benedetti, M. F.; van Riemsdik, W. H. *Environ. Sci. Technol.* **1996**, *30*, 1902−1910.
(51) Bhosle, N.; Suci, P. A.; Baty, A. M.; Weiner, R. M.; Geesey, G. G. *J. Colloid Interface Sci.* **1998**, *205*, 89−96.
(52) Hedrick, D. B.; Nivens, D. E.; Stafford, C.; White, D. C. *J. Microbiol. Methods* **1991**, *13*, 67−73.
(53) Nelson, W. H. *Modern techniques for rapid microbiological analysis*; VCH Publishers: New York, 1991.
(54) Williams, D. H.; Fleming, I. *Spectroscopic methods in organic chemistry*, 5th ed.; McGraw-Hill: London, 1995.
(55) Zeroual, W.; Manfait, M.; Choisy, C. *Pathol. Biol.* **1995**, *43*, 300−305.
(56) Wong, P. T. T.; Wong, R. K.; Caputo, T. A.; Godwin, T. A.; Rigas, B. *Proc. Natl. Acad. Sci. U.S.A.* **1991**, *88*, 10988−10992.